Analysis of air shower radio signals with REAS3

MARIANNE LUDWIG[1], TIM HUEGE[2]
[1]*Karlsruher Institut für Technologie, Institut für Experimentelle Kernphysik, Campus Süd, 76128 Karlsruhe, Germany*
[2]*Karlsruher Institut für Technologie, Institut für Kernphysik, Campus Nord, 76021 Karlsruhe, Germany*
marianne.ludwig@kit.edu
DOI: 10.7529/ICRC2011/V02/0149

Abstract: REAS3 is a new open-source Monte Carlo code using a universal endpoint formalism to describe and superpose the radio emission from single particles of an air shower. As it is based on CORSIKA simulations, the full complexity of air shower physics is taken into account. At the same time, REAS3 is a powerful tool for detailed studies of the radio emission characteristics and their relation to the underlying air shower properties. We discuss details of the simulated air shower radio pulses, in particular the pulse shapes at different observer positions and their relation to shower characteristics such as different particle energy regimes, phases of the air shower and the lateral distribution of particles.

Keywords: radio emission, extensive air showers, simulation, endpoint formalism

1 Introduction

In the last decade, the Monte Carlo code REAS [1] was investigated and developed further to simulate the **R**adio **E**mission from **A**ir **S**howers. Within REAS3, a universal endpoint formalism is used to calculate the emission of the complete air shower by superposing the radiation contributions of individual particles. Since REAS3 (as its former version REAS2 [2]) is based on COAST [3] histograms derived from CORSIKA [4], the full complexity of the underlying air shower is accounted for. Furthermore, with the endpoint formalism, all effects leading to radio emission are taken into account in a canonical way. For further details on REAS3 and the endpoint formalism, we kindly refer the reader to [5, 6, 7].

With REAS3, it is possible to study the radio pulse shapes and their relation to shower characteristics in detail. To achieve this, the particles of the air shower are categorized under several aspects, e.g. their energy or their atmospheric depth. For each category, its contribution to the complete radio signal is evaluated. Analysing the pulse shapes as done in the following section helps to understand how the particles of the chosen categories contribute to the radio signal.

2 Pulse shape analysis

A detailed study on the pulse shapes with REAS3 is possible, since REAS3 is using COAST [3] histograms derived from CORSIKA [4] simulations. In the histograms, the information on the particle distributions is saved and can be tracked through the complete air shower. For the analysis presented in this article, particles of the air shower are selected which fulfill a given criterion, e.g. the radio emission of particles in a specific energy range is calculated and compared with the emission of other energy ranges (cf. section 2.1). Already with REAS2, the details of the pulse shape have been analysed [2] in a similar fashion. For comparability, the categories and regions of the air shower development were chosen equal to the ones chosen for the REAS2 analysis. The analysis on the pulse shape was done at sea level for a vertical air shower with primary energy of 10^{17} eV and a magnetic field of 0.23 Gauss and -37° inclination, i.e. corresponding to the one at the Pierre Auger Observatory.

2.1 Particle energy

In this section, it is studied how particles with different energies contribute to the radio signal. Figure 1 shows the contributions of different particle energy regimes to the east-west polarisation where the radio pulse at 100 m north is on the top and at 400 m on the bottom. Close to the shower core, the particles with Lorentz factors between 10 and 100 dominate the radio signal. The particles with very small energies and Lorentz factors larger than 1000 contribute only little to the full radio signal. The particles with Lorentz factors between 10 and 100 and the particles with Lorentz factor between 100 and 1000 give roughly equal contributions to the overall radio pulse for the observer with 100 m distance. Although the particles with higher energies are fewer, the contribution is slightly larger, since beaming-effects lead to a more efficient radiation close to

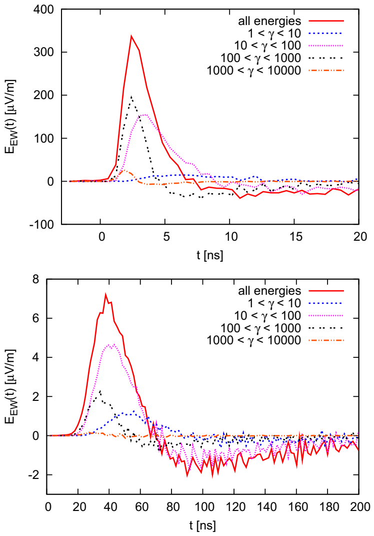

Figure 1: Contributions of different particle energy regimes to the east-west polarisation of the raw radio pulses for observers 100 m (top) and 400 m (bottom) north of the shower core.

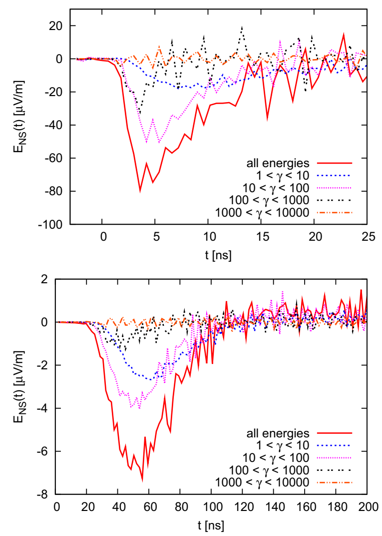

Figure 2: Contributions of different particle energy regimes to the north-south polarisation of the raw radio pulses for observers 100 m (top) and 400 m (bottom) north of the shower core.

the shower axis. Furthermore, close to the shower axis they are prominent.

However, this result is different from the one obtained with REAS2. With REAS2, the particles with a Lorentz factor between 100 and 1000 dominated strongly the signal at an observer distance of 75 m (cf. figure 24 in [2]). This implies that the endpoints of the particle trajectories contribute more efficiently at lower energies and less beamed than the pure geosynchrotron contributions considered in REAS2.

Comparing this with the contributions to the radio pulse at 400 m (bottom of figure 1), it is evident that particles with lower energies dominate the signal at larger distances. The particles with very large Lorentz factors do not contribute distinctly to the radio signal at this distance as it was true for REAS2 as well. This behaviour confirms that beaming effects influence the radio emission from air showers. For both observers, it is obvious that particles with different energies contribute at different times to the radio signal. The pulses for particles with higher energies have their maximum earlier than the pulses for low-energetic particles.

Figure 2 shows the contributions of different particle energy regimes to the north-south polarisation. (Please note the lower amplitudes for the observer at 100 m distance.) The radio pulse at 100 m north is on the top and at 400 m on the bottom. It is obvious that compared to the east-west polarisation, the lower energetic particles contribute more to the radio signal than high energetic particles. This is not surprising since the north-south polarised radio emission from a vertical air shower is arising purely from the charge excess in the air shower. The charge excess electrons mainly have lower energies because they originate from the atmosphere molecules from which they have been removed by ionisation and the corresponding positrons have been captured by negative charged ions in the atmosphere.

2.2 Lateral distance

To compare the contribution of different lateral distance ranges, the air shower has been split in rings. Since the radio signal scales with geometrical lengths and not with the atmospheric matter traversed, these rings are defined by geometrical distances independent of the atmospheric depth (and with this the density). Otherwise, the rings would have been defined dependent on the Molière radius. The result of the separation in geometrical cylinders is shown in figure 3. For small lateral observer distances, the particles close to the shower core mainly determine the signal. Particles which have a lateral distance larger than 100 m do not contribute to the observed radio signal at 100 m on ground. At this observer distance, the strongest emission comes from particles between 1 m − 10 m and 10 m − 100 m lateral distance. This is in agreement with the γ-distribution in the previous chapter, where the higher energetic particles dominate the radio signal close to the shower core and these particles are clustered close to the shower axis. At an observer distance of 400 m (bottom of figure 3), the radio signal is clearly dominated by the particles with lateral distances of 10 m − 100 m from the shower core. Only a small contribution is coming from the particles with lateral distances less than 10 m. The particles with distances larger than 100 m from the shower axis contribute very little to the radio signal at 400 m on ground. This is true for the observer at 100 m distance as well.

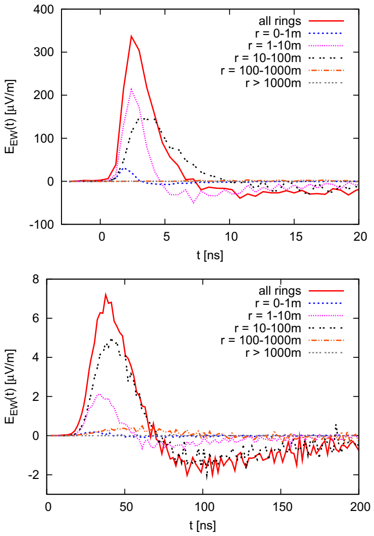

Figure 3: Contribution of different lateral rings to the east-west polarisation of the raw radio pulses for observers 100 m (top) and 400 m (bottom) north of the shower core.

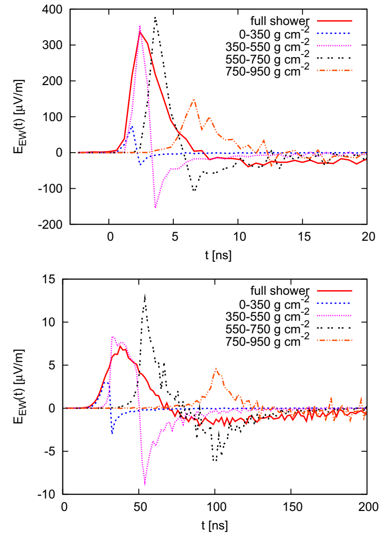

Figure 4: Contribution of different shower evolution stages to the east-west polarisation of the raw radio pulses for observers 100 m (top) and 400 m (bottom) north of the shower core.

The pure charge excess signal in the north-south polarisation component behaves similarly to the east-west polarisation component and therefore is not shown here. Comparing the results of this section with the previous results obtained with REAS2 [2], no major differences appear. This is well understood since the high energetic particles are clustered close to the shower axis and dominate the radio signal at small observer distances, while the signal at larger observer distances is dominated by the lower energetic particles from the cylinder with radius of $10 - 100$ m.

2.3 Shower Phase

Not only the contributions of particles with a specific energy or lateral distance are of interest, but also the contributions of different evolution phases of the air shower. To investigate this, the air shower has been divided in segments of atmospheric depth. Figure 4 displays the results for four different segments.

At first glance, one may wonder that the pulses of the individual slices overlap with each other and that the individual pulses are bipolar. This is mostly determined by the construction of the individual slices in the code. The layers are constructed in such way that the number of particles increases and decreases, thus each slice represents an own subshower which results in a bipolar pulse (for further details please see [9]).

The shower maximum of the extensive air shower considered in this section (and the previous and following sections) is at $689 \, \frac{\mathrm{g}}{\mathrm{cm}^2}$. Hence, the black curves represent the contributions of the slice including the shower maximum. For small observer distances, the radiation mainly comes from the regions around and before the shower maximum. For larger distances the region before the shower maximum dominates the signal, but the region around the shower maximum gives the largest positive contribution. This contribution is rather compensated by the radiation of the region before the shower maximum (cf. top of figure 4).

With REAS2, very similar results were obtained [2]. There, the emission was dominated by the shower phase around the shower maximum and the phase shortly before the shower maximum. Close to the shower core, the radiation of the different slices arrives nearly at the same time. With larger observer distances the arrival times get delayed due to geometrical effects. For smaller lateral distances, the geometrical time-delays are smaller. Considering a realistic refractive index in the atmosphere, the arrival times of the single pulses are expected to change at these distances and the radio pulse of the full shower will get narrower.

2.4 Geometric height

In conjunction with the previous section, it is interesting to look at the different regions of the air shower with respect to the geometrical height determining the radio physics instead of the atmospheric depth determining the air shower physics. To investigate this, the particles are equally chosen as in the previous section, while not the atmospheric depth is appointed but the height (in meters) above sea level. Figure 5 shows the contribution of the different heights above ground. Similar to the contributions of the atmospheric depths, the radio signals originating from the early phases (large heights) of the air shower arrive at first, then the others follow with decreasing height. The time-delay

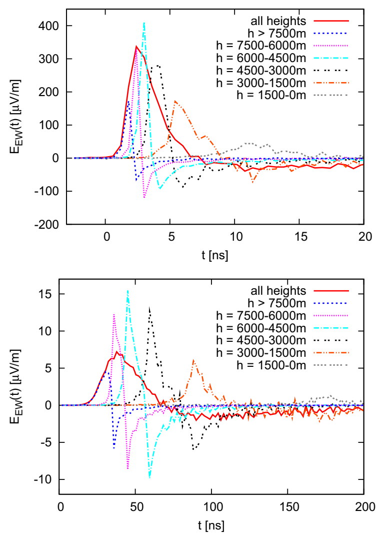

Figure 5: Contribution of different geometrical heights of the atmosphere to the east-west polarisation of the raw radio pulses for observers 100 m (top) and 400 m (bottom) north of the shower core.

of the single pulses is larger for increasing observer distances as well. Again, the pulses have an overlap due to the construction of the slices in the code. In contrast to the contributions of the different atmospheric depths, the maxima of the pulses from different geometrical heights are similar. This is consistent with the fact that geometrical scales determine the radio emission and not atmospheric scales. This is an important conclusion since it means that air shower physics can be decoupled from radio physics. For (air) shower physics the penetrated matter is crucial, e.g. for cross sections and interactions, whereas the quantities of radio physics such as the wavelength and light travel time depend on geometrical distances.

Moreover, particles below 1500 m do not contribute significantly to the overall radio signal, especially for the observer 400 m distant from the shower core. The results obtained in this section are comparable to the previous results obtained with REAS2. The charge excess component behaves similar to the one of the shower depth selection and thus, it is not shown here.

3 Conclusions and Outlook

With the results presented here, we analyzed the details and the influence of the shower development on the pulse shapes and showed that the pulse shape contains information on the shower development itself. In general, the previous results obtained with REAS2 were confirmed, but the relation of the charge excess pulse shape to the shower characteristics was studied for the first time.

With this understanding of the pulse shapes, the next step is to compare REAS3 with other models, in particular with an analytical approach which exhibits a simple correlation between pulse shape and shower development. Such a comparison is presented in [10]. Furthermore, comparisons between LOPES data and REAS3 simulations are studied and show a good agreement (cf. [11, 12, 13]). For the comparison with data, top-down simulations were developed based on a new version of CORSIKA [8] making a one-to-one comparison between the measured and simulated air shower and its radio emission possible by choosing showers reproducing the number of muons measured with KASCADE [9].

In the future, the influence of the refractive index of the atmosphere on the radio signal has to be studied, since in this analysis it is set to unity. In REAS3, a realistic refractive index is currently being implemented.

References

[1] T. Huege, H. Falcke, Astronomy & Astrophysics, 2005, **430**: 779-798

[2] T. Huege, R. Ulrich, R. Engel, Astrop. Phys., 2007, **27**: 392-405

[3] S. Lafèbre et. al., Astrop. Phys., 2009, **31**: 243-254

[4] D. Heck et. al., FZKA Report Forschungszentrum Karlsruhe, 1998, **6019**

[5] M. Ludwig, T. Huege, Astrop. Phys., 2010, **34**: 438-446

[6] M. Ludwig, T. Huege, Proceedings of the ARENA conference 2010, Nantes, France, NIM A, 2010, **in press**, doi:10.1016/j.nima.2010.10.115

[7] T. Huege, H. Falcke, C. W. James, M. Ludwig, these proceedings, **# 653**

[8] T. Pierog, these proceedings **#1170**

[9] M. Ludwig, PhD thesis, KIT, 2011, to be published

[10] M.Ludwig, T. Huege, O. Scholten, K. D. de Vries, these proceedings **#150**

[11] K. Link et al. (LOPES Collaboration), these proceedings **#404**

[12] N. Palmieri et al. (LOPES Collaboration), these proceedings **#309**

[13] F. Schröder et al. (LOPES Collaboration), these proceedings **#313**